High Fidelity MEMS Electrodynamic Micro-Speaker Characterization

E Sturtzer, I Shahosseini, Gaël Pillonnet, E Lefeuvre, G Lemarquand

High Fidelity MEMS Electrodynamic Micro-Speaker Characterization

E. Sturtzer,[1, a)] I. Shahosseini,[2] G. Pillonnet,[1, b)] E. Lefeuvre,[2] and G. Lemarquand[3]
[1)] *Institut des Nanotechnologies de Lyon (INL) – UMR CNRS 5270, Lyon, France*
[2)] *Institut d'Electronique Fondamental (IEF) – UMR CNRS 8622, Orsay, France*
[3)] *Laboratoire d'Acoustique de l'Universit du Maine (LAUM) – UMR CNRS 6613, Le Mans, France*

(Dated: 22 April 2013)

This paper deals with the heterogeneous characterization of a MEMS electrodynamic micro-speaker. This MEMS micro-speaker consists of an optimized silicon structure based on a very light but very stiff membrane. The mobile part is suspended using soft suspension beams, also made of silicon, which enable large out-of-plane displacement. The electromagnetic motor is composed of a micro-assembly permanent ring magnet and of a deposit mobile planar coil fixed on the top of the silicon membrane. Previous publications have presented the MEMS as theoretically able to produce high fidelity and high efficiency over a wide bandwidth. The present study intends to validate the electrical, the mechanical and the acoustic performance improvements. The characterization of the microfabricated micro-speaker showed that the electric impedance is flat over the entire audio bandwidth. Some results validates the performance improvements in terms of audio quality as compared to state of the art of the MEMS micro-speakers, such as the high out-of-plane membrane displacement over ± 400 μm, the 80 dB_{SPL} sound pressure level at 10 cm, the 2 % maximal distortion level, and the useful bandwidth from 335 Hz to cutoff frequency.

Keywords: acoustic transducers, electrodynamics, Micro-Electro-Mechanical Systems (MEMS), silicon micro-speaker, permanent magnet, planar electroplated copper microcoil, silicon beam, sound pressure level, total harmonic distortion

I. INTRODUCTION

The use of micro-speakers has significantly increased over the past few years in response to the flourishing market of mobile electronic devices with built-in audio systems. Mobile phones, tablets, GPSs are examples of devices with embedded micro-speakers which are used every day. The proposal made here is to take advantage of the MEMS (microelectromechanical system) technology to resolve the conflicting requirements of miniaturization and performance improvement: power efficiency, acoustic power, audio quality, and sound pressure level.

In the literature about MEMS, different actuation types are used for the micro-speakers. Among them, electromagnetic[1–3], piezoelectric[4], electrostatic[5] and magnetostrictive[6] are the most common. Though the piezoelectric and electrostatic ones are deployed more often than magnetostrictive and electromagnetic actuation because of the ease of microfabrication. But electromagnetic actuation has three major advantages regarding our application: high power density, low driving voltage and linear response.

This paper quantifies the improvements enabled by MEMS technologies in the case of a new structure of silicon micro-speaker. The authors have already described the MEMS process in[7,8]. Here, the paper focuses more on characterization of its performance, and after recalling the most important aspects of MEMS design, we present the practical characterization, i.e. electrical impedance, mechanical displacement, sensitivity, distortions (THD and IMD) and transient response.

II. MEMS DESIGN

In the case of the MEMS micro-speakers presented in most of the aforementioned work, the acoustic wave is generated using a deformable diaphragm, made of a deformable material such as parylene or polyimide[1,2]. In our work, both the membrane and the suspension are made of silicon. Silicon was chosen for the membrane because it fulfills both stiffness and lightness criteria. Its Young's modulus to density ratio of 71 GPa/(g/cm^3) is in fact three times higher than that of other materials commonly used in MEMS technology, such as titanium or aluminum. The sound wave is therefore generated by a rigid membrane covered by a thin latex film, resisting unwanted deformations and held by flexible suspension beams in monocrystalline silicon. This material was selected to be used for suspensions because of its linear stress-strain behavior and its outstanding fatigue life[9,10]. To have an idea of what an MEMS looks like, Fig. 1 illustrates a top view of the MEMS.

Development of new magnetic circuit is still a much-discussed topic[11]. For the proposed structure, the magnetic field is created by a ring-shaped magnet surrounding the circular membrane as micro-fabrication of magnets having a high magnetic field density is difficult even with today's technology. The conductor is a planar micro-coil wound on top of the membrane. The coil is

[a)] Author to whom correspondence should be addressed (eric.sturtzer@cpe.fr)
[b)] Second author to whom correspondence should be addressed (gael.pillonnet@cpe.fr)

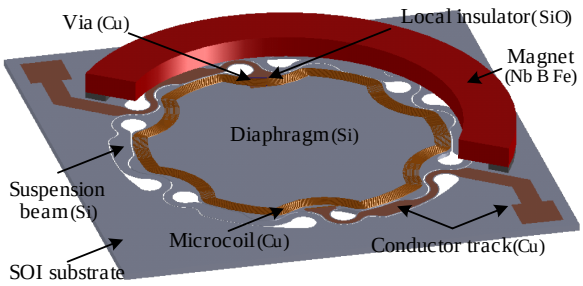

FIG. 1. Top view of the schematic structure of a MEMS micro-speaker.

placed as close as possible to the magnet in order to use the maximum intensity of the magnetic field. Its electrical supply is ensured using two conductive tracks which are supported by the suspension beams. Moreover, the coil is protected from short-circuits by an electrically insulating layer. Connections of the tracks to the coil ends are achieved through two vias across the insulating layer.

The first step in designing a loudspeaker is to determine the size and the displacement of the emissive surface (the membrane). These parameters are linked to the sound pressure level (SPL) and the frequency bandwidth. Subsections II A & II B detail the choices made in this work.

A. Membrane Design

At a given frequency f, for a loudspeaker which moves in piston mode the acoustic power is proportional to the displaced air volume. Both the membrane diameter (for a circular membrane) and the membrane out-of-plane displacement determine the air volume moved by the membrane. The target has been set to produce 80 dB_{SPL} at 10 cm, within a bandwidth (BW) of 300 Hz to 20 kHz. Therefore, for a membrane diameter, $\varnothing$, fixed to 15 mm, the maximum displacement, x_{peak}, is 300 μm (considered in section II B for the suspension springs design, and see[8] (Eq. (1))).

The dynamic performance was first analyzed on a thin silicon disc structure using finite element method (FEM) simulations. Taking a membrane with a thickness of 20 μm i.e. a membrane mass of 8 mg, the existence of more than 40 natural modes is detected in the microspeaker BW, with the drum mode at 1.3 kHz. This performance is very different from the expected one, i.e. too many structural modes in the targeted bandwidth.

To improve the stiffness of the membrane, without excessively increasing its mass, some ribs have been added (see Fig. 2). Thus, taking a plain membrane of 20 μm thick, but with 14 ribs each 300 μm thick and 150 μm wide, i.e. a membrane mass of 24 mg, there are only three modes (as presented in[8] (Fig. 5)) in the desired bandwidth, and the drum mode is shifted to 13 kHz. This solution is therefore a good trade-off between the sound quality (drum mode at 13 kHz and just three structural modes in the BW), the efficiency (membrane weight) and the microfabrication yield (considering the aspect and size ratio of the ribs). The rigid diaphragm is not sufficient to generate a piston movement. It is imperative for the suspension to be flexible and to provide large and linear out-of-plane displacements.

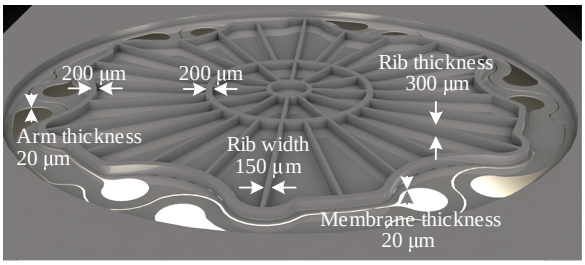

FIG. 2. Ribbed structure of the rear face of the silicon membrane.

B. Suspension Springs

Compared to the displacements usually considered in MEMS (a few microns), the $\pm$300 μm maximum displacement required for this application can be considered as a real challenge. In[8] and[12], different spring geometries were considered and the material maximum principal stress was analyzed in each case by finite element modeling (FEM). FEM static modeling enables the stress levels for 300 μm out-of-plane displacements for different spring shapes to be determined (Fig. 3).

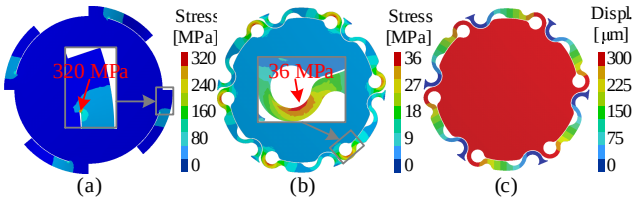

FIG. 3. Principal stress distribution (a)-(b); Out-of-plane displacement (c).

For the first design (Fig. 3a) we considered four simply curved suspension beams simply curved, clamped on one end into the substrate and on the other end into the membrane. Simulation results show that if the membrane is moved to its peak displacement of 300 μm, a 320 MPa maximal principal stress appears at the membrane-suspension anchorage zone. Although this value is lower than the theoretical elastic limit of a single silicon crystal (considered to be 7 GPa for (111) crystal orientation at room temperature[13]), the microfabricated prototype did not resist to the test bench (destruction of arm after few oscillations if the membrane is moved to its peak displacement). A safety factor of 10

(reduction of the maximum peak stress between the first and second prototype) was established to increase the micro-speaker resistance to unexpected operation and/or mechanical shock.

The second design (Fig. 3b) was also modeled, microfabricated and tested in order to verify the robustness and the linearity of the "U"-shaped beam. Static testing showed that it could stand more than 2 mm out-of-plane displacement. This is much more than in required in normal working conditions, but this ensures an appreciably large safety margin.

The stiffness of the suspension was set so that the piston mode frequency is under 300 Hz. FEM modal analyses of the membrane and the springs predicted that the piston mode frequency is at 35 and 75 Hz for four and six springs, respectively. Furthermore, this analysis showed that the drum mode frequency of the suspended membrane remains unchanged compared to the case of the free membrane studied in the previous subsection.

C. Copper Micro-Coil

Due to the micro-fabrication constraints, the coil with overlaid turns of the same diameter, commonly used in conventional micro-speakers, is replaced by a planar coil with concentric turns. In order to use the maximum intensity of the magnetic field, the coil turns are concentrated as much as possible on the periphery of the mobile part, close to the permanent magnet ring. The number of coil turns was set to maximize the electroacoustic efficiency while taking into account the technological limits. In this way, a 13-turn copper micro-coil, yielding almost the same mass as the silicon membrane, was electroplated. As Fig. 4 shows, each turn has a cross-section of $35 \times 30\ \mu m^2$ and a space of 20 μm with the juxtaposed turn. The micro-fabricated coil showed good thickness uniformity from the first interior turn to the first exterior turn, with a radius of 6.8 mm and 7.5 mm, respectively.

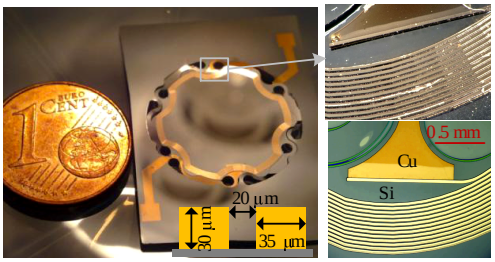

FIG. 4. Copper coil: microfabrication results.

D. Polarized Ring Permanent Magnet

The considered structure is a motor using only a one-ring radially-polarized permanent magnet. The configuration is shown in Fig. 5. Calculation of the magnetic field created by this permanent magnet, including the optimal dimensions (height, width and radii) and the optimal position relative to the micro-coil are presented in[14]. Note that calculations of the radial magnetic field are based on the Colombian model of a magnet[15]. As presented in subsection II C, the inner and outer radii for the coil, are 6.8 mm and 7.5 mm, respectively. For the magnet, the inner radius $r_{in} = 8$ mm. The outer radius, r_{out}, and the high, H, are to be defined. The magnet polarization, J, is 1.4 T and the moving coil is supposed to be flat.

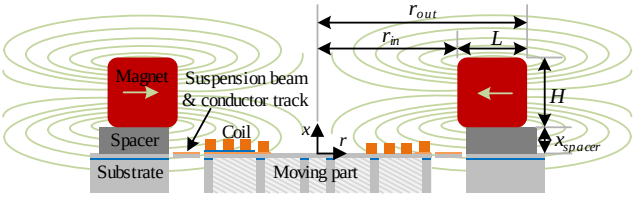

FIG. 5. Motor scheme using a radially-polarized ring permanent magnet.

As shown in Fig. 6, the radial magnetic field created by a ring permanent magnet of a given radius increases when the ring axial height, H, increases. However, according to[14], 3 mm seems to be the permanent magnet ring optimal axial height. Similarly, there is an interesting trade-off when the radial width, L, reaches 3 mm (Fig. 6). Indeed, smaller radial widths lead to a 40 % decrease in the radial field created. On the other hand, larger radial widths increase the field but the magnet volume becomes too great to be economically viable.

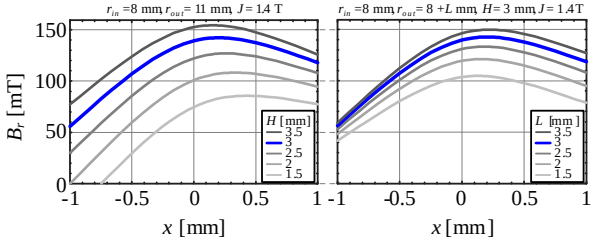

FIG. 6. Calculated radial magnetic field value, B_r, versus coil axial position, x, for several ring permanent magnet axial heights, H and radial widths, L.

From Fig. 6, it is clear that the radial magnetic field B_r is maximal if the coil is located 200 μm above the magnet upper face. Consequently, a spacer ($x_{spacer} = 200\ \mu$m) is used between the ring magnet and the substrate to locate the coil at this optimal axial position.

As shown in Fig. 7, the force factor is both high and uniform ($\Delta Bl \simeq 6$ %) for x varying from -100 μm to 500 μm, which corresponds to the excursion, x_{p-p}, of the moving coil in our prototype.

Finally, our chosen structure is a compromise between economics and size for a high magnetic field, and consists in a stator with only one axially polarized ring

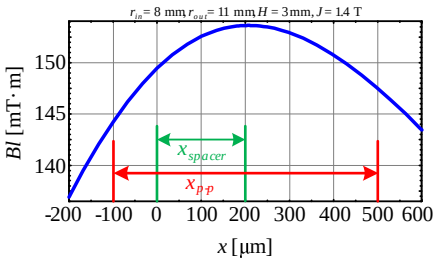

FIG. 7. Calculated force factor mean value, Bl, versus coil axial position, x.

permanent magnet (with $r_{in} = 8$ mm, $r_{out} = 11$ mm, $H = 3$ mm). This is an interesting trade-off as we obtain a relatively small magnet volume. The chosen permanent magnet material is neodymium-iron-boron grade $N52$, the strongest grade easily available on the market, with 1.45 T residual induction and 410 kJ/m^3 maximum energy product.

E. Final Result of the Design

The optimal configuration resulting from previous studies and discussion is given in Fig. 8, were on the left there is a top view of the MEMS and on the right the bottom view (microfabrication steps are presented in[7]). The membrane ribs are visible as well as the six U-shaped beams. Due to the form of the beams, the micro-coil is not perfectly circular. This choice was made so that the coil is immersed as much as possible in the highest part of the magnetic field.

FIG. 8. Photos of the MEMS micro-speaker.

III. CHARACTERIZATION OF THE MEMS

The essential parameters to describe the sound quality of the proposed MEMS loudspeaker are the impedance curve, frequency response, electro-acoustic efficiency, distortions and the transient response. The measurements were performed with different test benches (as shown in Fig. 9).

Since impedance is frequency dependent, a variable frequency generator is needed and AC level and phase meters are required to measure it (see Fig. 9a)). To make

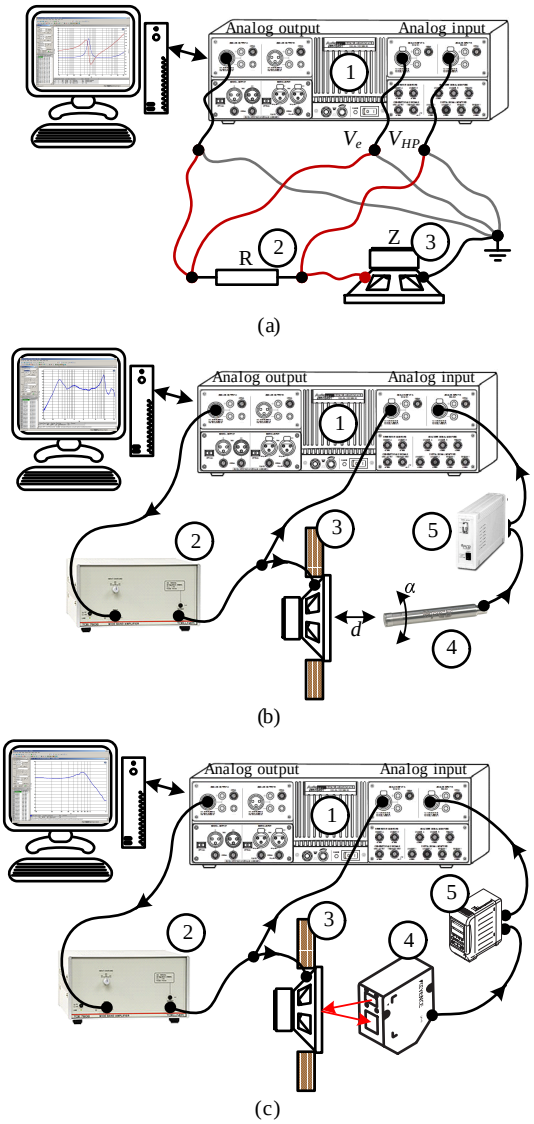

FIG. 9. Impedance (a), sound pressure level (b) and displacement (c) measurement setup.

audio-frequency impedance measurements, the adopted solution is an audio analyzer (*(1) Audio Precision SYS-2722*) wired to the device under test *(3)* and to a non-inductive resistor *(2)*.

For the acoustic measurements (Fig. 9b)), the same audio analyzer is used to generate the stimulus and to analyze the acoustic vibration, monitored by a microphone (*(4) PCB Piezotronics PCB378B02*) on the axis under free field conditions. A power amplifier (*(2) TOELLNER Test and Measurement TOE7608*) drives the MEMS for a high-fidelity electrical signal. An enclosure using an IEC 268-14 norm *(3)* is used to avoid acoustic short-circuits. The sound level is measured through a signal conditioner (*(5) PCB Piezotronics PCB482A21*) and was calibrated with a *Larson Davis CAL200* calibrator.

For the displacement measurements (Fig. 9c)), the

same power amplifier drives the MEMS and the same audio analyzer is used to generate the stimuli and to analyze the mechanical displacement. The displacement is determined by a laser (*(4) Keyence LK-G32* an optical triangulation position sensor) in a regular reflection setup monitored by a controller (*(5) Keyence LK-CD500*).

A. Impedance

The main electrical characteristic of a loudspeaker is its electrical impedance over frequency. This impedance helps choose the audio amplifier in order to match it to the loudspeaker. The electric impedance modulus and phase angle of the MEMS micro-speaker for a large bandwidth is shown in Fig. 10a. Unlike standard micro-speakers the modulus response of the MEMS is flat ($|Z| = 13.4\ \Omega \pm 0.5\ \%$) over the entire audio BW (see Fig. 10b). With a maximum phase shift of 3 °, it is almost a flat response for the phase angle, φ. The MEMS loudspeaker exhibits a low resonance peak at $F_S = 335$ Hz, allowing an easier amplifier design than for standard micro-speakers.

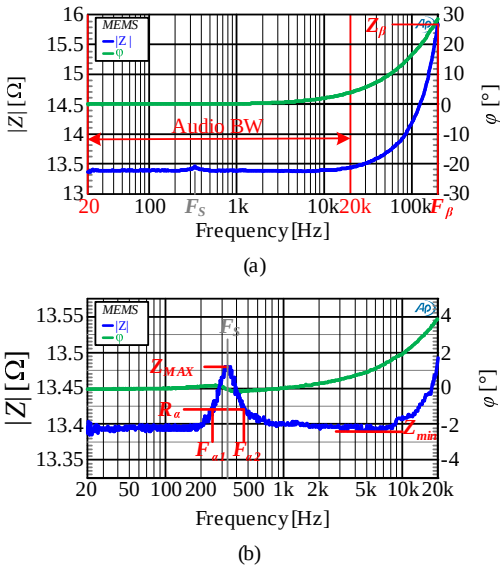

FIG. 10. Electric impedance modulus, $|Z|$, and phase angle, φ, versus frequency.

B. Thermal aspect

The thermally-limited power capability is 60 A/mm^2, linked to the voice-coil sizing (cf. Fig. 11, heating does not exceed 10 °/W thanks to the large heat exchange surfaces). These limitations have to be taken into account when selecting the amplifier.

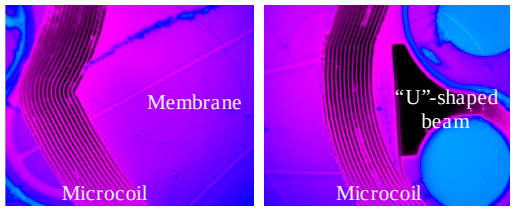

FIG. 11. MEMS thermal picture which illustrates the large heat exchange surfaces and the low heating of the coil.

C. MEMS Equivalent Circuit

To model the MEMS in order to design the associated audio amplifier, the small signal equivalent circuit is given in Fig. 12a and the electrical equivalent circuit is given in Fig. 12b. The reference model has been established by[16] and is still a much-discussed topic[17,18]. The parameters of interest are: the voice coil inductance, L_e, the DC resistance of the voice coil, R_e, the moving mass, m_m, the mechanical resistive losses, r_m, and the suspension compliance, c_m. Note that the eddy current resistance, R_μ, is neglected and that the radiation resistances, R_{av} and R_{ar} are far below r_m so are also neglected and do not appear in the electrical schematics and equations.

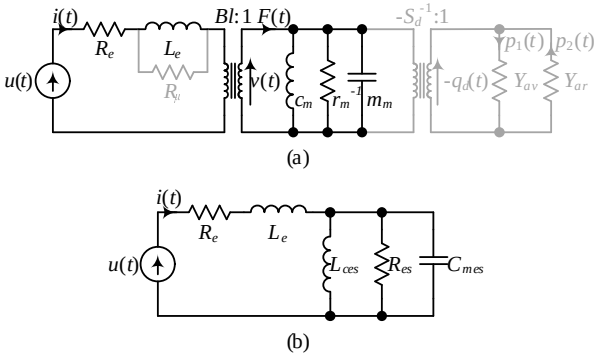

FIG. 12. Equivalent circuits of a drive unit : (a) Electrical-mechanical-acoustic equivalent circuit; (b) Simplified electrical equivalent circuit.

The small signal parameters are the calculations of R_e, L_e, R_{es}, C_{mes} and L_{ces} and are based on Eqs. (1) (see[16,19–21]). The maximal and minimal impedance modulus are equal to $|Z_{MAX}| = 13.46\ \Omega$ and $|Zmin| = 13.39\ \Omega$, respectively (see Fig. 10b). Based on Eq. (1b), $R_\alpha = 13.42\ \Omega$ and the two frequencies where $|Z|$ is equal to R_α are $F_{\alpha 1}$ and $F_{\alpha 2}$ (272 Hz and 420 Hz, respectively). F_β is set as high as possible so that the loudspeaker is in the inductive area. At $F_\beta = 200$ kHz, $|Z_\beta|$ is equal to 15.9 Ω (see Fig. 10a).

$$R_e = |Z_{\min}| \tag{1a}$$

$$R_\alpha = R_e\sqrt{r_0} = |Z_{\min}|\sqrt{|Z_{MAX}|/|Z_{\min}|} \tag{1b}$$

$$L_e = \frac{\sqrt{|Z_\beta|^2 - |Z_{\min}|^2}}{2\pi F_\beta} \tag{1c}$$

$$R_{es} = |Z_{MAX}| - |Z_{\min}| \tag{1d}$$

$$C_{mes} = \frac{\sqrt{|Z_{MAX}|/|Z_{\min}|}}{2\pi\left(F_{\alpha 2} - F_{\alpha 1}\right)\left(|Z_{MAX}| - |Z_{\min}|\right)} \tag{1e}$$

$$L_{ces} = \frac{\left(F_{\alpha 2} - F_{\alpha 1}\right)\left(|Z_{MAX}| - |Z_{\min}|\right)\sqrt{|Z_{\min}|/|Z_{MAX}|}}{2\pi F_{\alpha 1} F_{\alpha 2}} \tag{1f}$$

Moreover, as m_m is estimated at 35 mg and knowing Eqs. (2a)–(2c), it is possible to determine Bl, r_m and c_m. The values of the different elements composing the two equivalent circuits are listed in Table I. By measuring the non-linearities, these parameters could be used to determine the large signal behavior of the micro-speaker[18] or to determine the most suitable type of control[22].

$$m_m = C_{mes} \times (Bl)^2 \tag{2a}$$

$$c_m = L_{ces} \Big/ (Bl)^2 \tag{2b}$$

$$r_m = (Bl)^2 \Big/ R_{es} \tag{2c}$$

TABLE I. The values of the different elements composing the two equivalent circuits.

Parameter	Value	Unit
R_e	13.39	Ω
L_e	6.82×10^{-6}	H
R_{es}	0.07	Ω
C_{mes}	15.4×10^{-3}	F
L_{ces}	14.4×10^{-6}	H
Bl	47.7×10^{-3}	T · m
m_m	31×10^{-6}	kg
r_m	325×10^{-3}	kg/s
c_m	6.3×10^{-3}	m/N

D. Membrane Displacement

Fig. 13 shows the measurement of the applied force versus displacement and using this figure and $F = \xi \times K$, the stiffness has been estimated at 6.4 N/m.

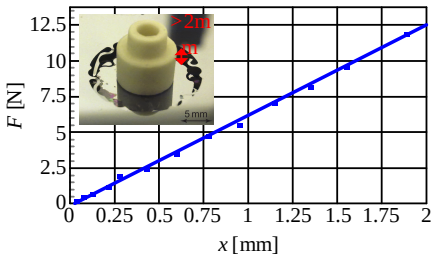

FIG. 13. Force applied versus displacement.

1. Quality Factor

The equations for the mechanical, electrical and total quality factors (Qms, Qes and Qts, respectively) are presented in Eqs. (3a)–(3c)[19]. Qms, Qes and Qts are equal to 2.27, 2.26 and 1.13 respectively. As the total quality factor is greater than 0.7, the MEMS is an under-damped system. We therefor expect to find a peak near the resonance frequency in the displacement response.

$$Q_{ms} = \frac{F_S \times \sqrt{r_0}}{F_{\alpha 2} - F_{\alpha 1}} \tag{3a}$$

$$Q_{es} = \frac{Q_{ms}}{r_0 - 1} \tag{3b}$$

$$Q_{ts} = \frac{Q_{ms} \times Q_{es}}{Q_{ms} + Q_{es}} \tag{3c}$$

2. Displacement Response

The average displacement position of the membrane is sensed by using laser equipment in a regular reflection setup (given in Fig. 9b). The Fig. 14 shows the normalized function of the displacement of the moving part mounted on an infinite baffle (0 dB = 100 μm). As expected in section III D 1, the overshoot of x near F_S, confirms that the total quality factor is greater than 0.7. At F_S, $|x|$ = 2.4 dB equivalent to Qts = 1.3 (slightly higher than the 1.13 expected from the theory).

In section II B, the peak displacement limit was estimated at ±300 μm. The measurements showed over ±400 μm displacement without mechanical and electrical failure.

As the diaphragm diameter, ∅, is 15 mm (see section II A), the surface, S, is 176.7 mm^2 and the maximum displacement volume is $Vd = 2 \times x_{peak} \times S \simeq 140$ mm^3 (at F_S = 335 Hz). In the state of the art[23,24], the maximum displacement volume for MEMS micro-speaker applications is around 4 mm^3 at 1 kHz (a significantly higher frequency). This comparison of volume of air displaced

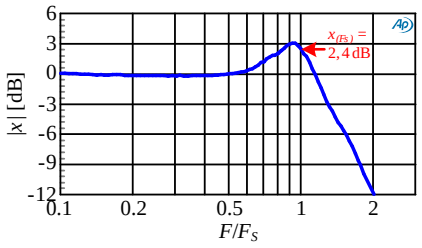

FIG. 14. Normalized displacement versus frequency.

(140 mm^3 versus 4 mm^3) highlights the technological leap achieved in this study (significant displaced air volume at low frequencies = possibility to generate bass with a high sound level).

E. Transient Response

The displacement response, $x(t)$, of the MEMS to a voltage step input is plotted in Fig. 15a. Measurements were performed with a *Tektronix DPO 2014* oscilloscope, coupled with a *Tektronix TCP0030* current probe and a *LK-G32* laser. The displacement response is a good way to observe the quality factor of the MEMS. As expected in section III D 1, the MEMS is an under-damped system: the overshoot of $x(t)$ (see Fig. 15b), confirms that the total quality factor is greater than 0.7.

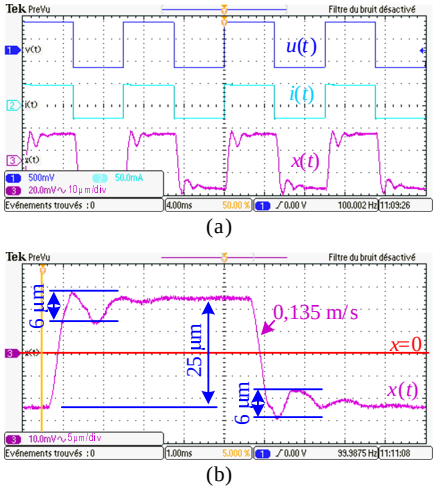

FIG. 15. Transient plot of the voltage $v(t)$, the current $i(t)$ and the membrane displacement $x(t)$.

F. Sound Pressure

The frequency response is given because it is closely correlated to the perceived sound quality. The Fig. 16 shows the radiated acoustic power, L_P, versus frequency of the MEMS device (measured as shown in Fig 9a). The microphone has first been placed in $d = 1$ cm ($\alpha = 0$ °) and the driver delivers 100 mW and then $d = 10$ cm ($\alpha = 0$ °) and $P_{elec} = 1$ W. The measured characteristic pressure is 79 dB in 10 cm. The MEMS behaves as a wideband loudspeaker. The curve presents a resonance frequency at 335 Hz as predicted in the design stage. The BW is significantly larger than previous MEMS micro-speakers and also larger than current micro-speakers used in mobile phone applications[25]. The upper part of the response shows relatively smooth resonances due to the rigidity of the silicon membrane. The relatively flat response gives non-colored sound in free field conditions. This response has a significant peak at around 9 kHz, due to a natural frequency caused by the ≈ 90 μm thick latex film (added to avoid sound leakage).

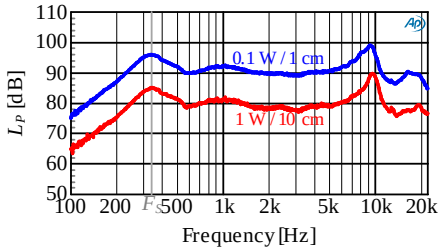

FIG. 16. MEMS sound pressure level response of an infinite baffle micro-speaker system.

G. Electro-acoustical Efficiency

The loudspeaker efficiency is the ratio between the acoustic power delivered and the electrical power received by the loudspeaker. The electrical power has been found from the impedance and the input voltage of the MEMS loudspeaker. The microphone measurement gives the sound pressure level which can be converted into acoustic power by the following equation:

$$P_{acou} = 10^{\frac{L_P}{10}} \times P_0 \times 4\pi d^2 \qquad (4)$$

where $P_0 = 10^{-12}$ W is the reference acoustic power and d the measurement distance (MEMS is considered to be a piston which acts as a punctual source i.e. $d > \varnothing$). The measured characteristic sensitivity for $1W_{(elec)}$ is 79 dB in 10 cm. By using Eq. (4), it is possible to deduce that $Pacou = 10$ μW.

As efficiency is the ratio of acoustic power to electrical power, the MEMS achieves 1×10^{-3} % efficiency ($\equiv 59$ dB$_{\text{SPL}}$ calculated for 1 W in 1 m). Compared to existing loudspeakers in mobile applications, the proposed device has a similar efficiency but with a larger BW (with a lower frequency limit ≈ 335 Hz instead of ~ 650 Hz). The tradeoff between BW and efficiency by changing the size of the device (of the mobile mass) could be done to fit the MEMS performance to a specified application. The efficiency can also be increased by choosing a stronger magnet, but this is not a cost effective solution.

H. Total Harmonic Distortion

Harmonic distortion is an indicator characterizing the effects of nonlinearities. Fig. 17 presents a frequency spectrum at $F = 750$ Hz with an acoustic power sweep ($75 < L_P < 95$ dB). Note that for better readability, the curves have been slightly shifted in frequency. Additional measurement was performed to confirm that the distortion coming from the amplifier is negligible. The distortion level is around -40 $dB_{(SPL)}$ for H2 and -55 $dB_{(SPL)}$ for H3. The MEMS therefor introduces less disturbing distortions than existing micro-speakers. Different sinusoidal excitations have been applied to the MEMS device and the results lead to the same conclusion.

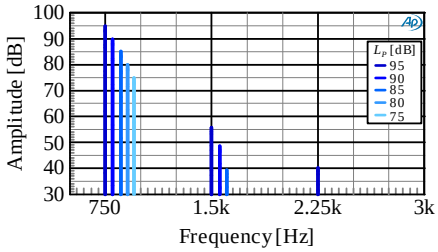

FIG. 17. FFT at 750 Hz for different sound pressure levels, L_P.

Fig. 18 shows the THD vs. frequency, and as can be seen, the distortion is lower than 0.1 % in the entire audio band and lower than 0.016 % for frequencies higher than 200 Hz, allowing the use in the high end mobile application.

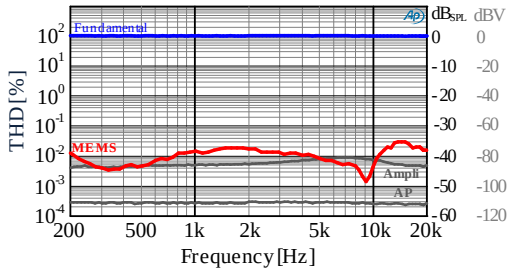

FIG. 18. THD versus frequency ($P_{elec} = 250$ mW).

I. Intermodulation Distortion (IMD)

Intermodulation performance is related to the ability of the speaker to restore different tones from signals composed of individual frequencies. Fig. 19 provides an example of measurement with a two-tone stimulus applied to the MEMS. F_1 represents an "instrument" tone and F_2 represents a "voice" tone, both chosen inside the flat band of the MEMS sensitivity curve (Fig. 16). Note that in this test, the amplitude of the instrument is four times lower than the voice tone ($\Delta v = 12$ dBV), to have a realistic example of typical sound.

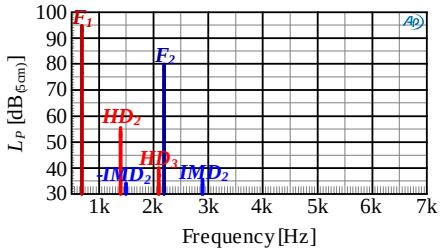

FIG. 19. IMD spectrum of the MEMS loudspeaker ($F1 = 700$ Hz and $F2 = 2.2$ kHz).

As can be seen from the above figure, the amplitudes of the IMD are very low (see $-IMD2$ and $IMD2$) or absent (no-third order intermodulation or at least less than 50 dB relative to the amplitude of the voice tone). The distortion that should be created by the voice tone (e.g. at $2 \times F2$ or $3 \times F2$) is also less than 50 dB compared to the amplitude of the voice tone and less than 65 dB compared to the amplitude of the instrument tone.

Additional measurements with a two-tone stimulus, such as bass-sweep, voice sweep and frequency difference have also been performed and give similar results. These measurements indicate that the loudspeaker behaves correctly, i.e. the MEMS loudspeaker gives a relatively clear distinction between tones (listening tests also confirm this feeling).

IV. CONCLUSION

The present heterogeneous characterization of the proposed electrodynamic micro-speakers validates the improvement introduced by the MEMS approach compared to standard micro-speakers. The silicon structure based on a light and stiff membrane is well suited to acoustic emission and efficiency. The mobile part is suspended with soft silicon suspension beams, allowing a large out-of-plane displacement, unparalleled for MEMS technology and enabling a large sound level to be produced. The electromagnetic motor composed of a micro-assembly permanent ring magnet and a deposited mobile planar coil has been optimized for linear and power efficient displacement. This combination provides a MEMS micro-speaker with a 79 dB measured pressure level in 10 cm, 335 Hz cut-off frequency, less than 0.016 % THD and 59 dB_{SPL} calculated nominal characteristic sensitivity for 1 W in 1 m. The proposed MEMS could therefor be an attractive solution compared to the current micro-speakers and to the state of the art of the MEMS micro-speakers especially for the large bandwidth and the high sound volume.

ACKNOWLEDGMENTS

This work was financially supported by the French National Research Agency (ANR).

[1]M.-C. Cheng, W.-S. Huang, and S. R.-S. Huang, Journal of Micromechanics and Microengineering **14**, 859 (2004).
[2]S.-S. Je, F. Rivas, R. Diaz, J. Kwon, J. Kim, B. Bakkaloglu, S. Kiaei, and J. Chae, Biomedical Circuits and Systems, IEEE Transactions on **3**, 348 (2009).
[3]Y. Chen and Y. Cheng, in *Micro Electro Mechanical Systems (MEMS), 2011 IEEE 24th International Conference on* (2011) pp. 1213–1216.
[4]S. H. Yi and E. S. Kim, Japanese Journal of Applied Physics **44**, 3836 (2005).
[5]H. Kim, A. Astle, K. Najafi, L. Bernal, P. Washabaugh, and F. Cheng, in *Sensors, 2005 IEEE* (2005) p. 4 pp.
[6]T. S. Albach, P. Horn, A. Sutor, and R. Lerch, J. Appl. Phys. **109**, 07E510 (2011).
[7]I. Shahosseini, E. Lefeuvre, M. Woytasik, J. Moulin, X. Leroux, S. Edmond, E. Dufour-Gergam, A. Bosseboeuf, G. Lemarquand, and V. Lemarquand, in *Sensors, 2010 IEEE* (2010) pp. 2426–2430.
[8]I. Shahosseini, E. Lefeuvre, E. Martincic, M. Woytasik, J. Moulin, S. Megherbi, R. Ravaud, and G. Lemarquand, Microsystem Technologies **18**, 1791 (2012).
[9]M. Legros, O. Ferry, F. Houdellier, A. Jacques, and A. George, Materials Science and Engineering: A **483–484**, 353 (2008), 14th International Conference on the Strength of Materials.
[10]Y. Chida, H. Katsumata, T. Fujiya, S. Kaihatsu, T. Morita, D. Hoshino, and Y. Nishioka, Sensors and Actuators A: Physical **169**, 367 (2011).
[11]C.-M. Lee, J.-H. Kwon, G.-Y. Hwang, and S.-M. Hwang, J. Appl. Phys. **105**, 07E710 (2009).
[12]I. Shahosseini, E. Lefeuvre, E. Martincic, M. Woytasik, J. Moulin, S. Megherbi, R. Ravaud, and G. Lemarquand, in *Design, Test, Integration and Packaging of MEMS/MOEMS (DTIP), 2011 Symposium on* (2011) pp. 258–262.
[13]S. Franssila, *Introduction to Microfabrication*, 2nd ed. (Wiley, 2010).
[14]G. Lemarquand, R. Ravaud, I. Shahosseini, V. Lemarquand, J. Moulin, and E. Lefeuvre, Applied Acoustics **73**, 379 (2012).
[15]R. Ravaud and G. Lemarquand, Progress In Electromagnetics Research (2009), 10.2528/PIER09042105.
[16]R. H. Small, J. Audio Eng. Soc **20**, 383 (1972).
[17]J. H. Huang, H.-C. Her, Y. C. Shiah, and S.-J. Shin, J. Appl. Phys. **103**, 033502 (2008).
[18]W. Klippel, in *Audio Engineering Society Convention 133* (2012).
[19]C. J. Struck, in *Audio Engineering Society Convention 82* (1987).
[20]R. Gomez-Meda, in *Audio Engineering Society Convention 91* (1991).
[21]W. Waldman, in *Audio Engineering Society Convention 94* (1993).
[22]E. Sturtzer, G. Pillonnet, G. Lemarquand, and N. Abouchi, Applied Acoustics **73**, 1087 (2012).
[23]S.-S. Je and J. Chae, Electron Device Letters, IEEE **29**, 856 (2008).
[24]F. Neri, F. Di Fazio, R. Crescenzi, and M. Balucani, in *Electronic Components and Technology Conference (ECTC), 2011 IEEE 61st* (2011) pp. 1221–1227.
[25]Y. C. Shiah, H.-C. Her, J. H. Huang, and B. Huang, J. Appl. Phys. **104**, 104905 (2008).

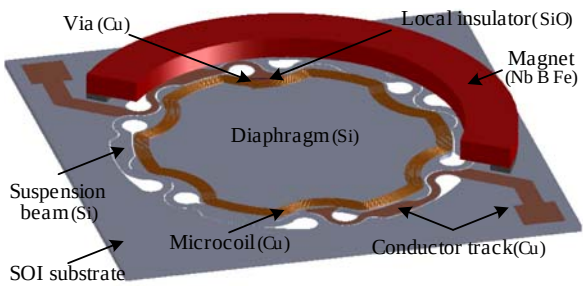
Via (Cu)
Local insulator (SiO)
Magnet
(Nb B Fe)
Diaphragm (Si)
Suspension
beam (Si)
Microcoil (Cu)
Conductor track (Cu)
SOI substrate

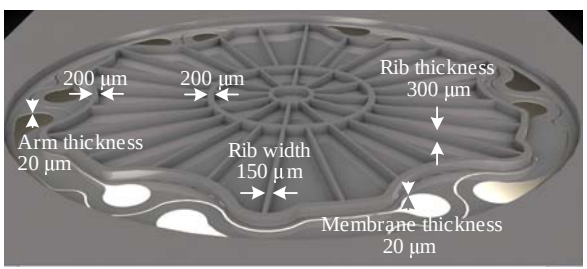
200 µm
200 µm
Rib thickness
300 µm
Arm thickness
20 µm
Rib width
150 µm
Membrane thickness
20 µm

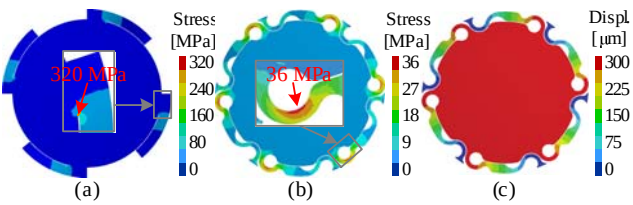
320 MPa
Stress
[MPa]
320
240
160
80
0
36 MPa
Stress
[MPa]
36
27
18
9
0
Displ
[µm]
300
225
150
75
0

(a) (b) (c)

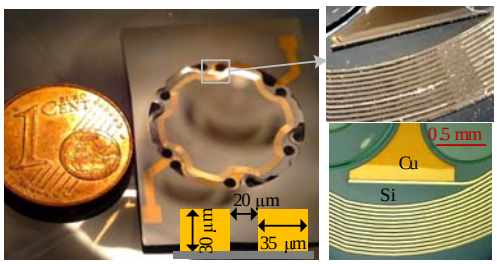
20 µm
30 µm
35 µm

0.5 mm
Cu
Si

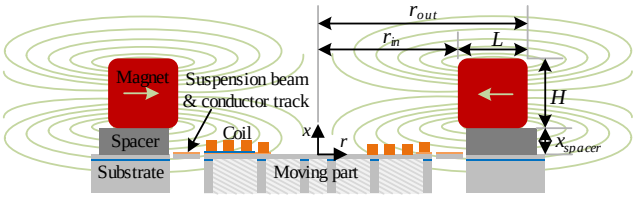
r_{out}
r_{in}
L
H
Magnet
Suspension beam
& conductor track
Coil
Spacer
Substrate
Moving part
x
r
x_{spacer}

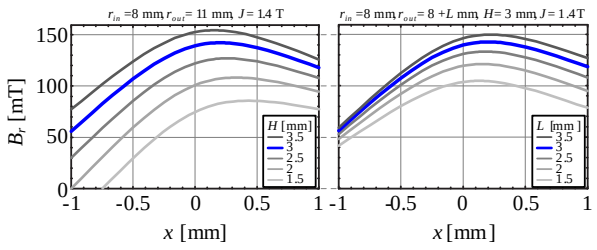
r_{in} =8 mm, r_{out}= 11 mm, J= 1.4 T
r_{in} =8 mm, r_{out}= 8 +L mm, H= 3 mm, J= 1.4 T
B_r [mT]
150
100
50
0
-1
-0.5
0
0.5
1
x [mm]
H [mm]
3.5
3
2.5
2
1.5
L [mm]
3.5
3
2.5
2
1.5

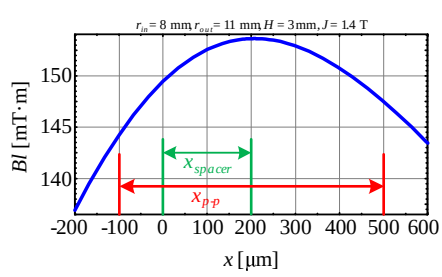
r_{in} = 8 mm, r_{out} = 11 mm, H = 3 mm, J = 1.4 T
150
145
140
Bl [mT·m]
x_{spacer}
$x_{p\text{-}p}$
-200 -100 0 100 200 300 400 500 600
x [µm]

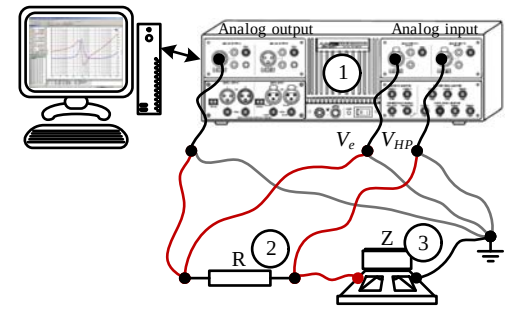
Analog output
Analog input
1
V_e
V_{HP}
R
2
Z
3

(a)

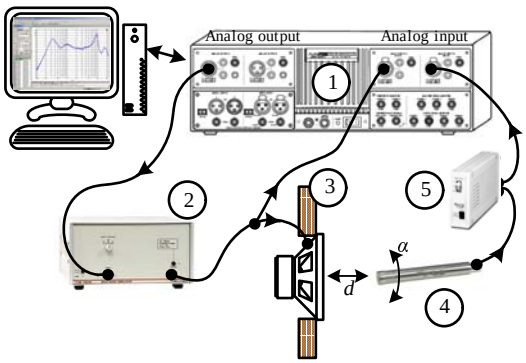
Analog output
Analog input
1
2
3
5
α
d
4

(b)

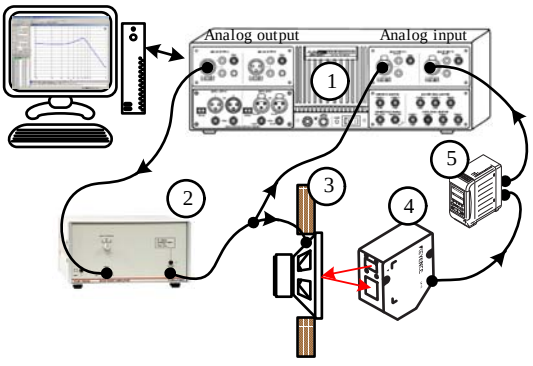
Analog output
Analog input
1
5
2
3
4

(c)

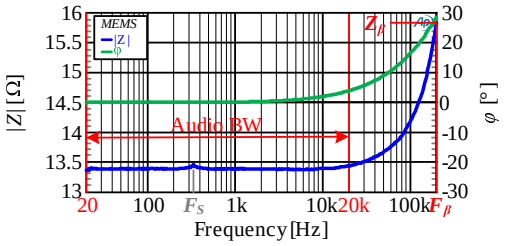
MEMS
|Z|
ϕ
16
15.5
15
14.5
14
13.5
13
30
20
10
0
-10
-20
-30
|Z| [Ω]
φ [°]
Audio BW
Z_β
F_β
F_S
20
100
1k
10k
20k
100k
Frequency [Hz]

(a)

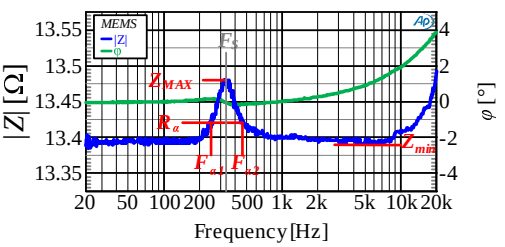
MEMS
|Z|
ϕ
13.55
13.5
13.45
13.4
13.35
4
2
0
-2
-4
|Z| [Ω]
φ [°]
F_S
Z_{MAX}
R_α
Z_{min}
$F_{\alpha 1}$
$F_{\alpha 2}$
20
50
100
200
500
1k
2k
5k
10k
20k
Frequency [Hz]

(b)

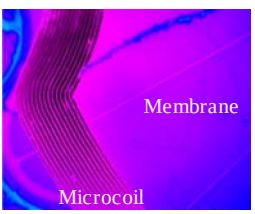
Membrane
Microcoil

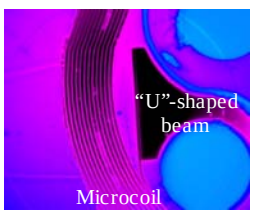
“U”-shaped
beam
Microcoil

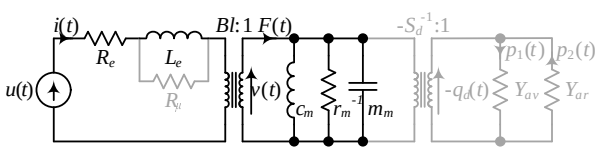
i(t)
Bl:1 F(t)
-S_d^-1:1
R_e
L_e
u(t)
R_fe
V(t)
c_m
r_m
m_m
p_1(t)
p_2(t)
-q_d(t)
Y_av
Y_ar

(a)

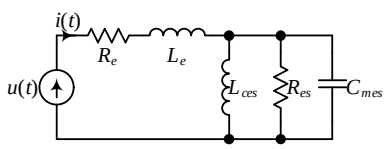
i(t)
R_e
L_e
u(t)
L_ces
R_es
C_mes

(b)

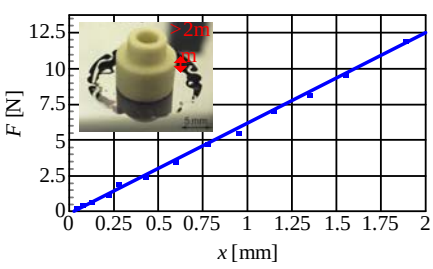
12.5
10
7.5
5
2.5
0
F [N]
0
0.25
0.5
0.75
1
1.25
1.5
1.75
2
x [mm]

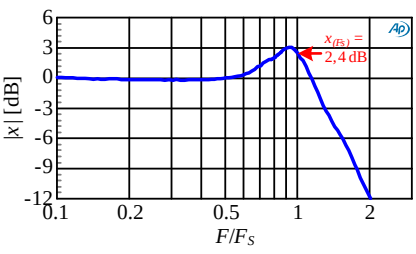
6
3
0
-3
-6
-9
-12
|x| [dB]
0.1
0.2
0.5
1
2
F/F_S
x(F3) =
2,4 dB

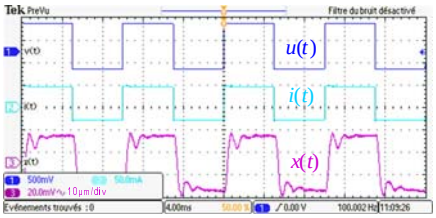
Tek PreVu
Filtre du bruit désactivé
u(t)
i(t)
x(t)
500mV
20.0mV/∿ 10 µm/div
Evénements trouvés : 0
4.00ms
0.00 V
100.002 Hz
11:09:26

(a)

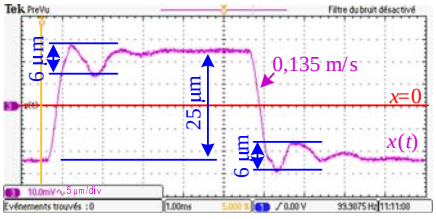
Tek PreVu
Filtre du bruit désactivé
6 µm
0,135 m/s
25 µm
x=0
6 µm
x(t)
10.0mV/∿ 5 µm/div
Evénements trouvés : 0
1.00ms
0.00 V
93.3875 Hz
11:11:08

(b)

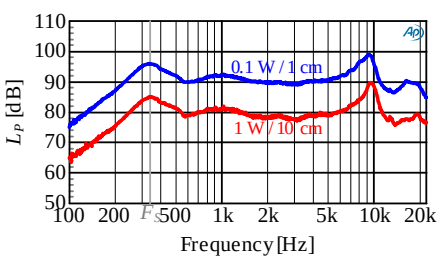
110
100
90
80
70
60
50
L_p [dB]
0.1 W / 1 cm
1 W / 10 cm
100
200
F_S
500
1k
2k
5k
10k
20k
Frequency [Hz]

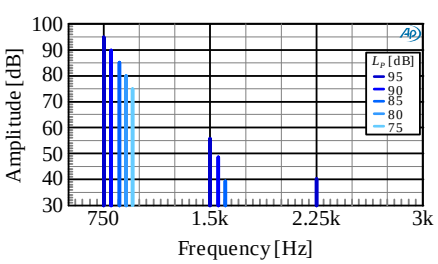
100
90
80
70
60
50
40
30
Amplitude [dB]
750
1.5k
2.25k
3k
Frequency [Hz]
L_p [dB]
95
90
85
80
75

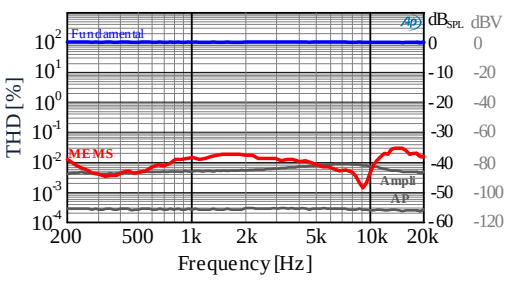
dB$_{SPL}$
dBV
Fundamental
MEMS
Ampli
AP
THD [%]
Frequency [Hz]
200
500
1k
2k
5k
10k
20k

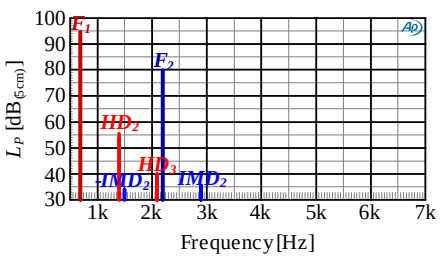
100
90
80
70
60
50
40
30
L_P [dB$_{(5\,cm)}$]
F_1
F_2
HD_2
HD_3
IMD_2
IMD_2
1k
2k
3k
4k
5k
6k
7k
Frequency [Hz]